Highly conductive epitaxial ZnO layers deposited by atomic layer deposition

Zs. Baji[1], Z. Lábadi[1], Gy. Molnár[1], B. Pécz[1], K. Vad[2], Z. E. Horváth[1], P.J. Szabó[3], T. Nagata[4], J. Volk[1],

[1]Research Centre for Natural Sciences Institute for Technical Physics and Materials Science Konkoly Thege M. út 29-33, H-1121 Budapest, Hungary

[2]Institute of Nuclear Research of the Hungarian Academy of Sciences (ATOMKI) P.O. Box 51, H-4001, Debrecen, Hungary

[3] Budapest University of Technology and Economics, Műegyetem rkp. 3-9. H-1111 Budapest, Hungary

[4] International Center for Materials Nanoarchitectonics (WPI-MANA), National Institute for Materials Science, 1-1 Namiki, Tsukuba 305-0044 Japan

E-Mail: baji.zsofia@ttk.mta.hu

The possibility of depositing conductive epitaxial layers with atomic layer deposition has been examined. Epitaxial ZnO layers were grown on GaN and doped with Al. The resistivity of the epitaxial layers is between 0.6 and $2*10^{-4}$ Ωcm with both the mobilities and the carrier concentrations very high. The source of the high carrier concentration was found to be a combination of Al and Ga doping, the latter resulted by Ga atoms diffusing into the ZnO from the GaN substrate.

Keywords: ALD, ZnO, conductive, epitaxy, Ga doping

1. Introduction

Atomic layer deposition (ALD) is a self limiting layer growth method based on the chemisorption and reaction of precursor gases on a heated substrate. Between the precursor pulses, the reactor is purged with an inert gas. As the precursors can only react with the substrate surface and never with one another in gas phase, the growth occurs monolayer by monolayer, and an epitaxial growth can easily be achieved. The chemisorption also ensures the uniform and conformal coverage independent of the surface morphology. [1-5]

ZnO has recently attracted considerable attention because of its versatility in a number of applications, such as sensors and photovoltaic devices [6,7]. It can be doped with aluminium to increase its conductivity, and be used as transparent conductive oxide layer [8-10]. The ALD method for ZnO deposition is widely known and has a great variety of applications [11-14.] as the layers are transparent, and even the intrinsic layers have a low resistivity (~10^{-2}-10Ωcm), which can be further reduced by Al doping.

Epitaxial ZnO layers have been grown with a number of methods [15-17], the mobility of these layers was typically between 10 and 100 cm^2/Vs and the carrier concentrations around 10^{17}-$10^{20}/cm^3$. There have been a few reports on conductive epitaxial ZnO layers doped with Ga or Al [18,19]. The growth of ALD deposited monocrystalline layers has been proved to be possible as well [20-23], but the conductivity of these layers has not been examined.

The motivation for this research was the need for conductive epitaxial layers for the purpose of seed layers for exciton based solar cells and for ZnO nanowire based lasers. High quality epitaxial n-type doped layers with tunable resistivity are very promising materials for next generation UV light emitting diodes or laser diodes. On the one hand they could be the active layers, or they could serve as template layers as a good alternative for very expensive ZnO single crystals.

Our previous experiments [24] on the nucleation of ZnO showed that an epitaxial growth is

possible at 300°C deposition temperature, but not at 220°C, which would be favourable, as the ZnO layers with the best conductivities were deposited at and under this temperature [25]. The aim of this work was therefore to deposit conductive epitaxial layers at different deposition temperatures and doping conditions. According to Kim et al. [26] an in-diffusion of the substrate atoms to the ALD grown film is possible, therefore it is possible that diffusing Ga atoms could serve as electrically active dopants. Ga is an even more effective dopant in ZnO than Al. Both Al and Ga diffuse in ZnO with a substitutional mechanism. In the temperature range of 750-1000°C the solubility of aluminium in zinc oxide is $n = 1.0 \times 10^{23} \exp(-1.08\ k^{-1}T^{-1})$ ions/ cm^3 and the solubility of gallium is $n = 2.7 \times 10^{21} \exp(-0.59 k^{-1}T^{-1})$ ions/ cm^3, where the activation energies are in eV. The diffusion is dependent on their surface concentration, and their diffusion coefficients are $D = 5.3 \times 10^{-2} \exp(-2.74\ k^{-1}T^{-1})\ cm^2\ sec^{-1}$ for Al, and $D = 3.6 \times 10^{4} \exp(-2.74\ k^{-1}T^{-1})\ cm^2\ sec^{-1}$ for Ga. On the other hand an additional Al doping was applied to see if the conductivity can be further increased, and the effect of the doping on the epitaxial growth.

2. Experimental

ZnO layers were deposited in a Picosun SUNALE TM R-100 type ALD reactor. The Zinc precursor was Diethyl-zinc (DEZ) and the oxidant was H_2O vapour. The precursors were electronic grade purity and kept at room temperature. The carrier- and purging gas was 99.999% purity nitrogen. During deposition the pressure in the chamber was 15 hPa. The flow rates were 150 sccm. The pulse time of all precursors was 0.1 s, the purging times were 3 s after each DEZ, and 4 s after the water pulses.

The substrates were 6 μm thick GaN layers epitaxially grown on sapphire substrates. The substrates were cleaned in acetone, ethylene and high purity water.

The ZnO layers were deposited at temperatures between 150°C and 300°C. Double layers were also grown with a thin (20 nm) layer grown at 300°C and a thicker (35 nm) at 210°C. It was expected that the epitaxial buffer layer grown at 300°C would force the top layer to also grow epitaxially, and the layers grown at 210°C have previously proved to be conductive. Therefore these layers were expected to be epitaxial with a fairly low resistivity. Aluminium doped samples were also prepared at those deposition temperatures where epitaxial growth was achieved. The list of the prepared samples is presented in table 1 and 2.

After the layer deposition the resistivity of a number of layers was measured. Contacts were fabricated on these samples with silver paste, and were reinforced with glue. The back side of the samples was cleaned with HCl, so that the layer would only be on the top side of the GaN, and the contacts would be placed on the actual edge of the layer. The resistivities were measured in the Van der Pauw configuration.

The thickness of the samples was measured with a profilometer. The specific resistivities and the mobilities were calculated using these measured thickness values.

Crystal structure and orientation was examined by X-ray diffraction (XRD) carried out on a Bruker AXS D8 Discover diffractometer equipped with Göbel mirror, using a scintillation counter and Cu Kα radiation. High resolution triple crystal X-ray diffractometry (TCD) analyses were performed on the samples for the evaluation of the epitaxial fit of the layers to the substrate using the same X-ray diffractometer equipped with asymmetric Ge (022) 4-bounce primary monochromator and 3-bounce Germanium 022 channel cut analyzer monochromator. For reciprocal space mapping measurements (RSM), a 1 dimensional position sensitive detector (Bruker Vantec-1) and monocromated Cu Kα radiation with a Ge 002 monochromator crystal were employed.

Transmission electron microscopic (TEM) imaging was performed in a Phillips CM 20 TEM with a tungsten electron gun operated between 20 and 200kV. High resolution images were

made in a JEOL 4000EX microscope operating with a LaB6 electron source between 80 and 400kV accelerating voltage. The images were recorded with a Gatan CCD camera. Electron backscatter diffraction (EBSD) measurements were performed by a Philips XL-30 type scanning electron microscope supplied with an EDAX-TSL EBSD-system.

The depth profiles were measured by an INA-X type scanning neutral mass spectroscopy (SNMS) equipment by Specs GmbH, Berlin. Inductively coupled low-pressure radio frequency Ar plasma was used to provide both sample bombardment and post ionization. The sputtered particles were identified with a quadruple mass spectrometer with a secondary electron multiplier. The concentrations were determined using relative sensitivity factors of the constituents. The sputtering time was converted to depth scale from sputtering rates determined by a high-sensitivity surface profiler.

3. Results and discussion

3.1 The deposition of epitaxial layers

The deposition of epitaxial layers was attempted at temperatures varying between 150°C and 300°C. The crystallinity of the layers was determined with XRD. The measured Θ/2Θ curves of three representative samples deposited at 150°C, 220°C and 300°C are presented in Fig 1.a. The XRD patterns of the samples are dominated with the strong GaN (001) substrate peak at 2Θ = 34.56° which almost perfectly overlaps with the ZnO (002) peak at 2Θ = 34.421°. The results show that the intrinsic ZnO layers grown at 150 and 210°C have both (002) and (101) peaks. The Θ/2Θ curves of the samples deposited above 270°C show no additional peaks to that of the GaN substrate. This leads to the conclusion that if they are crystalline, they have an epitaxial structure following the (001) orientation of the GaN substrate. All the layers possessed the typical peaks presented in Fig.1.a. In the case of the films deposited under 270°C the (101) peak of ZnO at 2Θ = 36.252° is also apparent while

neither the (100) at 2Θ = 31.769° nor the (102) at 2Θ = 47.568° was observed showing that these layers are not epitaxial, but only some specific orientations are present. To make sure that the layers deposited at higher temperatures are indeed epitaxial, high resolution TCD measurements were conducted near the GaN (002) peak, these results are presented in Fig. 1.b. This method made it possible to resolve the ZnO (002) peak (at cca 34.42°) beside that of the GaN at 34.563. In the case of the doped ZnO layers the peak has shifted towards higher angles (to cca. 34.75°) due to the decreased lattice constant resulted by the substitution of the Zn atoms with the smaller Al atoms in the ZnO lattice.

To further examine the crystalline quality, regular and high resolution TEM images were taken on the intrinsic ZnO layer grown at 300°C. These images can be seen in Fig. 2.a and 2.b. The TEM micrographs clearly reflect that the ZnO film followed the structure of the GaN substrate precisely. The films are high quality and epitaxial.

Reciprocal space mapping of the (104) lattice point was also conducted on the samples deposited at 270 °C, and the intrinsic double layer. These maps are presented in fig. 3.a. and b. Figure 3.a. shows a (104) reflection by the RSM of the samples deposited at 270 °C, indicating an asymmetric peak along the Qx-axis. The peak corresponds to the GaN substrate. To investigate the peak position of the ZnO layer in detail, cross sectional analysis of the RSM was performed as shown in Fig. 3.a.(i) and (ii). Dashed lines in Fig 3.a. are picked up positions of the Qz (i) and Qx (ii). Both the Qz (i) and Qx (ii) are asymmetric peaks as indicated by the blue arrows. The peaks were fitted with two peaks using the literature value of GaN (c=0.519 and a=0.319; ref. international center for diffraction data. PDF-2 card 50-0792). From these results, the lattice parameters of ZnO could be determined, and found to be c=0.520±0.001 and a=0.321±0.001 nm. As these values are a little bit smaller than the literature value (c=0.521 and a=0.325; ref. international center for diffraction data. PDF-2 card 36-1451), the ZnO layer is relaxed. The intrinsic double layer also showed the

same tendency as the samples deposited at 270 °C as shown in fig. 3b.

3.2 The effect of the Al doping on the crystallinity

The effect of the doping was examined at all the growth temperatures where an epitaxial growth was experienced. Therefore Al doped samples were prepared at 270°C and 300°C growth temperatures, and a doped double layer was also deposited with a 20 nm buffer layer deposited at 220°C and a 2at % Al doped top layer at 300°C. The crystalline quality of the doped layers has also proved to be very good. These layers are still highly oriented, continuous and uniform but they are not perfectly epitaxial any more. They appear oriented in the (001) direction, but they also have peaks at $2\Theta = 31.77°$ and 36,25° displaying the (100) and the (101) reflections of ZnO, respectively. This shows that even though these layers are not polycrystalline, they must contain crystallites with orientations other than that of the GaN substrate. The XRD results from the layers are presented in table 1.

Somewhat contradictory to the XRD findings, a (104) reflection by the RSM of the doped double layer as same tendency as the samples deposited at 270 °C as shown in fig. 4a. Therefore to determine if the doped samples are still mainly highly oriented with some crystallites in other orientations, or they are completely polycrystalline, in other words, to see, how much of the surface of the layers was oriented differently, EBSD experiments were conducted. The result of the ZnO film deposited at 300°C and doped with 2% Al is presented in Fig. 4.b. It can be seen that most of the sample surface shows a (002) orientation following the crystalline orientation of the GaN substrate. Only small domains have the c axis parallel to the surface.

3.3 The conductivity of the films

The list of the deposited layers and their measured resistivities, carrier concentrations and the

calculated mobility values are listed in table 2. The resistivity of the GaN layer under the ZnO films was six orders of magnitude higher than that of the ZnO, therefore their contribution to the conduction could be neglected.

The resistivities of all the samples were very low. The mobility values are very high, compared to the literature values listed above, these are around the maximum achievable mobility values for epitaxial ZnO films. The carrier concentrations are also very high, already in the undoped layers. One possibility to explain this high value of carrier concentration was to suppose that the intrinsic doping, that is, the oxygen vacancies, zinc interstitials and hydrogen doping, was so high in these layers. This is somewhat in contrast with the high crystalline quality of the layers, as these unintentional dopants in ZnO are contaminations and defects that would deteriorate the crystallinity of the layers. This points towards the conclusion that the Ga atoms did diffuse into the ZnO films. The depth profile of the layers was measured and the Ga diffusion was indeed found. The measurements are presented in Fig. 5. The straight line shows simulation results of the elemental distribution in case of no inter-diffusion [27.] It can be seen, that the zinc, oxygen and nitrogen concentrations are in fact on this line, whereas the Ga diffused into the ZnO layer. The Ga concentrations are between 1% (near the interface) and 0.01% (on the front side, near the middle).

To evaluate this hypothesis a thicker (70 nm) intrinsic ZnO film was also deposited at 300°. The resistivity of this layer is higher and the carrier concentration is lower than those of the thinner layers, as the Ga could not diffuse into the whole thickness of the layer. The resistivities of the deposited films vs. the thicknesses are shown in fig. 6. It can be seen, that the Ga doping efficiency decreases with the thickness of the film, but an additional Al doping can further decrease the resistivity values.

4. Conclusions

High quality epitaxial ZnO layers were deposited with ALD. The layers deposited at 270°C

and above tend to be epitaxial, but an epitaxial seed layer deposited at high temperatures ensures that the top layer grown at lower temperatures also grows epitaxially. In the case of the Al doped layers small domains with a different orientation also appeared.

All the layers had high conductivities. This was resulted by the high mobility due to the excellent crystalline structure and the high carrier concentrations. The latter is mainly caused by the diffusion of Ga atoms into the layer, and an additional Al doping can further reduce the resistivity, although not significantly.

References

[1] S.M. George, Atomic Layer Deposition: An Overview, Chem. Rev. 110 (2010) 111-131.

[2] M. Ritala, M. Leskela, Atomic layer epitaxy - a valuable tool for nanotechnology? Nanotechnology 10 (1999) 19-24

[3] H. Kim, H. B. R. Lee, W. J. Maeng, Applications of atomic layer deposition to nanofabrication and emerging nanodevicesThin Solid Films 517 (2009) 256-2580

[4] M. Ritala, M. Leskela, Atomic layer deposition (ALD): from precursors to thin film structures, Thin solid Films 409 (2002) 138-146.

[5] T. Suntola J. Hyvarinen, Atomic layer epitaxy, Annu. Rev. Mater. Sci. 15 (1985) 177-195

[6] C. Jagadish, S. J. Pearton (Eds.) Zinc Oxide Bulk, Thin Films and Nanostructrues, Elsevier, 2006

[7] T. Tynell, M. Karppinen, Atomic layer deposition of ZnO: a review, Semicond. Sci. Technol. 29 (2014) 043001-0430016

[8] J.W. Elam, S.M. George, Growth of ZnO/Al2O3 Alloy Films Using Atomic Layer Deposition Techniques, Chem.Mater. 15 (2003) 1020-1028

[9] C. H. Ahn, H.Kim, H.K. Cho, Deposition of Al doped ZnO layers with various electrical types by atomic layer deposition, Thin Solid Films, 519 (2010) 747-750.

[10] S.D. Kirby, R.B van Dover, Improved conductivity of ZnO through codoping with In and Al, Thin Solid Films 517 (2009) 1958-1960.

[11.] E. H. Kim, D. H. Lee, B. H. Chung, H. S. Kim, Y. Kim and S. J. Noh, Low-Temperature Growth of ZnO Thin Films by Atomic Layer Deposition, Journal of the Korean Physical Society, 50. (2007) 1716-1718

[12.] A. Yamada, B.Sang, M. Konagai, Atomic layer deposition of ZnO transparent conducting oxides, Appl. Surf. Sci. 112 (1997) 216-222

[13] J.Lim, C. Lee, Effects of substrate temperature on the microstructure and photoluminescence properties of ZnO thin films prepared by atomic layer deposition Thin Solid Films 515 (2007) 3335-3341.

[14] S. J.Lim, S.Kwon, H. Kim, ZnO thin films prepared by atomic layer deposition and rf sputtering as an active layer for thin film transistor Thin Solid Films 516 (2008) 1523-1528

[15] B.M. Ataev, A.M. Bagamadova, V.V. Mamedov , A.K. Omaev, Thermally stable, highly conductive, and transparent ZnO layers prepared in situ by chemical vapor deposition, Materials Science and Engineering B65 (1999) 159–163

[16] J. Zhao, L. Hu, Z. Wang, Z. Wang, H. Zhang, Y. Zhao, X. Liang, Epitaxial growth of ZnO thin films on Si substrates by PLD technique, Journal of Crystal Growth 280 (2005) 455–461

[17] M. Kumar, R.M. Mehra, S-Y. Choi, Current Applied Physics 9 (2009) 737–741

[18] R. M. Ataev, A. M. Bagamadova, A. M. Djabrailov, V. V. Mamedov, R. A. Rabadanov, Highly conductive and transparent Ga-doped epitaxial ZnO films on sapphire by CVD Thin Solid Films, 260 (1995) 19 -20

[19] Z. Zhang, C. Bao, S. Ma, S. Hou, Applied Surface Science 257 (2011) 7893-7899

[20] H.C. Chen, M.J. Chen, T.C. Liu, J.R. Yang, M. Shiojiri, Structure and stimulated emission of a high-quality zinc oxide epilayer grown by atomic layer deposition on the sapphire substrate, Thin Solid Films 519 (2010) 536-540

[21] L. Wachnicki, T. Krajewski, G. Luka, B. Witkowski, B. Kowalski, K. Kopalko, J.Z. Domagala, M. Guziewicz, M. Godlewski, E. Guziewicz, Monocrystalline zinc oxide films grown by atomic layer deposition , Thin Solid Films 518 (2010) 4556-4669

[22] J. Lim, K. Shin, H. Woo Kim, C. Lee, Effect of annealing on the photoluminescence characteristics of ZnO thin films grown on the sapphire substrate by atomic layer epitaxy, Materials Science and Engineering B 107 (2004) 301-304

[23] C.S.Ku, J-M. Huang, C.M. Lin, H.Y. Lee, Fabrication of epitaxial ZnO films by atomic-layer deposition with interrupted flow, Thin Solid Films 518 (2009) 1373-1376

[24] Zs. Baji, Z. Lábadi, Z.E. Horváth, Gy. Molnár, P. Barna, Nucleation and Growth Modes of ALD ZnO, Cryst. Growth Des. 12. (2012) 5615-5620.

[25] Zs. Baji, Z. Lábadi, Z. E. Horváth, M. Fried, B. Szentpáli, I. Bársony, Temperature dependendent in situ doping of ALD ZnO, J Therm Anal Calorim, 105 (1) (2011) 93-99

[26] S.K.Kim, C.S. Hwang, S.-H. K. Park, S.J. Yun, Comparison between ZnO films grown by atomic layer deposition using H2O or O3 as oxidant, Thin solid films 478 (2005) 103-108

[27] B. G. Attolini, C. Ferrari, C. Frigeri, M. Calicchio, F. Rossi, K. Vad, A. Csik, Z. Zolnai, Effect of temperature on the mutual diffusion of Ge/GaAs and GaAs/Ge, Crystal Growth 318. (2011) 367-371

Figures and tables:

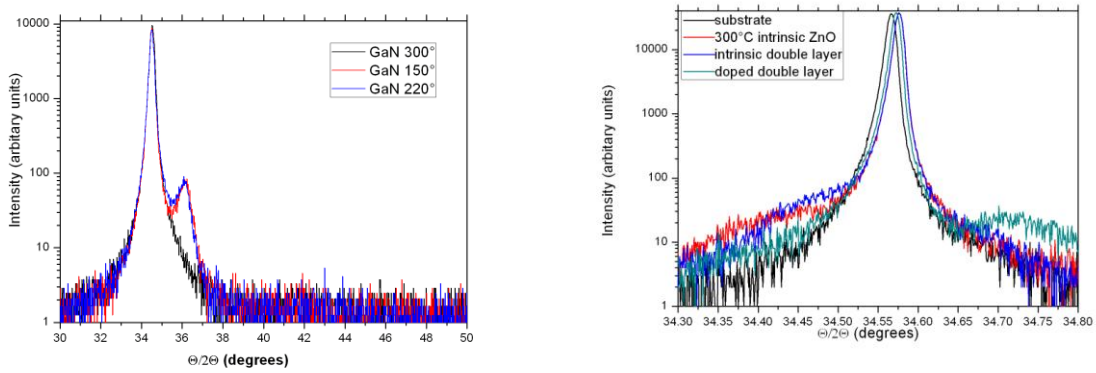

Figure 1. XRD Θ/2Θ spectra of the samples deposited at 150, 220 and 300°C (a), and the TCD spectra of the 300°C intrinsic, the intrinsic double layer, the doped double layer and the GaN substrate around the (002) diffraction peak

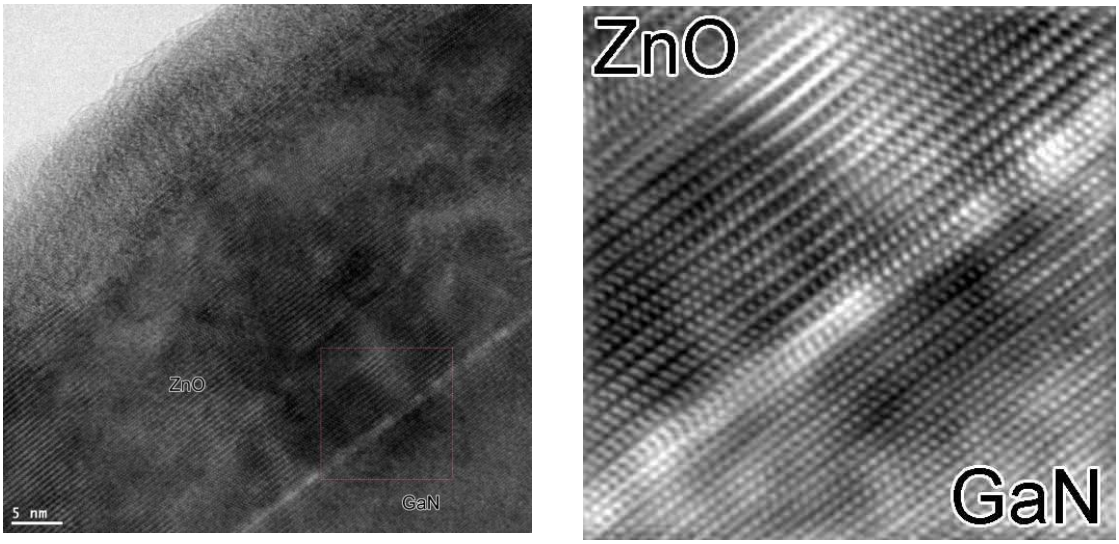

Fig. 2. a and b: The TEM micrograph and the high resolution TEM image taken on the sample deposited at 300°C

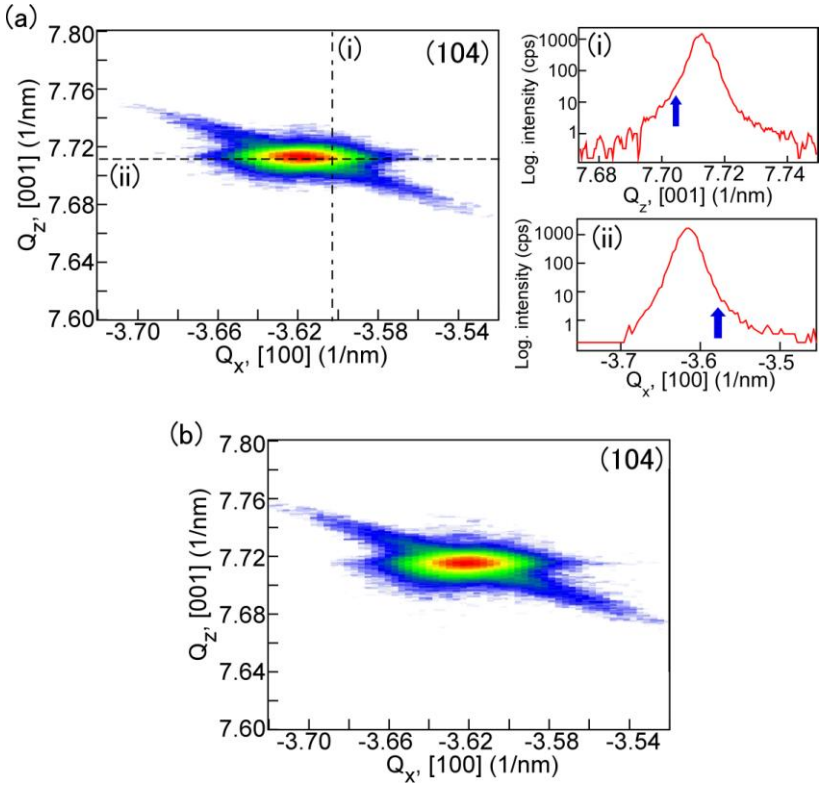

Fig. 3. The reciprocal space map of the epitaxial ZnO layer grown at 270°C (a), with the cross sectional analysis of this asymmetrical peak (a i and ii) and the intrinsic double layer (b)

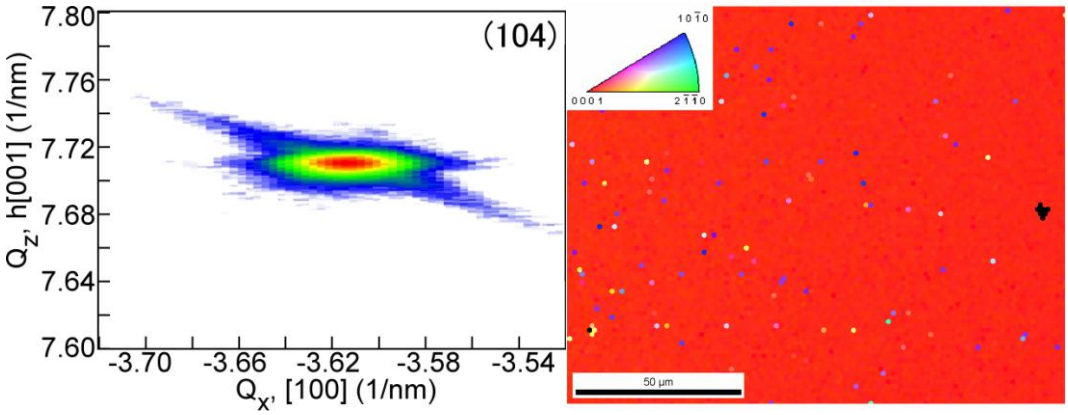

Fig. 4.a and b. the reciprocal space map and the EBSD map of the double layer doped with 2% Al, respectively

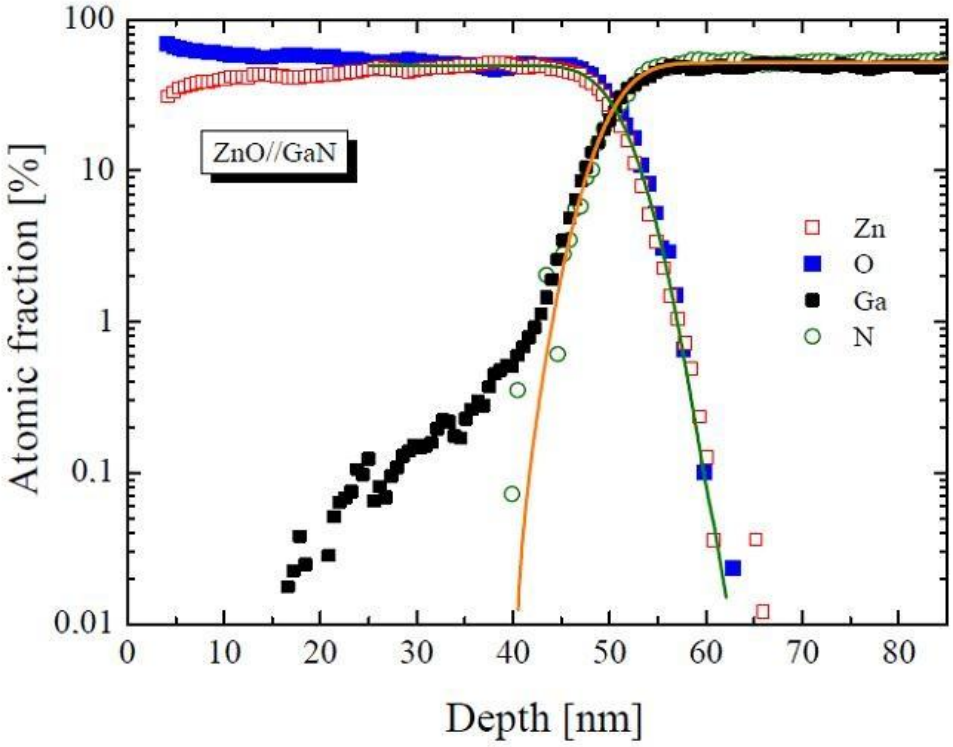

Fig. 5. The depth profile of the layers as measured by SNMS whith simulation results showing the case of no inter-diffusion (straight line)

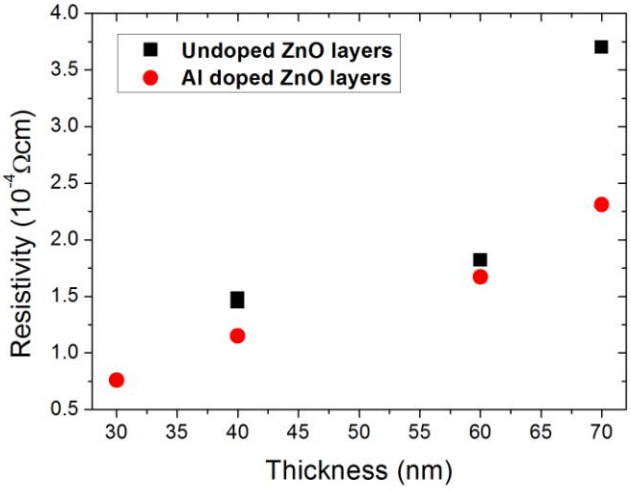

Fig 6. The resistivities of the doped (circles) and undoped (squares) layers plotted against the film thickness

Prepared layers	XRD results
150°C	(001) oriented, but a small (101) peak also apparent
220°C	(001) oriented, but a small (101) peak also apparent
300° intrinsic	Epitaxial in the (001) orientation
270° intrinsic	Epitaxial in the (001) orientation
Buffer+ intrinsic top layer	Epitaxial in the (001) orientation
Buffer + 2% doped top layer	(001) oriented, but a small (100) peak also apparent
270° doped with 1.6 at% Al	(001) oriented with both (100) and (101) peaks
300° doped with 2 at% Al	(001) oriented, but a small (101) peak also

Table 1. The XRD results of the ZnO samples

Prepared layers	Thickness	ρ (10^{-4}Ωcm)	μ (cm^2/Vs)	n (10^{20}/cm^3)
300° doped with 2 at% Al	30 nm	0.76	140.3	5.8
Buffer + 2% doped top layer	60 nm	1.67	109.8	3.4
270° doped with 1.6 at% Al	40 nm	1.15	104.4	5.2
270° intrinsic	40 nm	1.45	122.4	3.5
Buffer+ intrinsic top layer	60 nm	1.82	118.2	2.9
300° intrinsic	40 nm	1.48	131.2	3.2
300° intrinsic	70 nm	3.7	112.3	1.5

Table 2. The layers with their resistivities, carrier concentrations and mobilities